

PAPR and BER Analysis in FBMC/OQAM System with Pulse Shaping Filters and Various PAPR Minimization Methods

Allanki Sanyasi Rao¹, Madhu Kumar Vanteru², Azmera Chandu Naik³, Karthik Kumar Vaigandla⁴,
Radha Krishna Karne⁵

¹Associate Professor, Department of ECE, Christu Jyothi Institute of Technology and Science, Jangaon, Telangana, India

^{2,4}Assistant Professor, Department of ECE, Balaji Institute of Technology and Science, Warangal, Telangana, India

³Senior Assistant Professor, Department of ET[AIML], CVR College of Engineering, Rangareddy, Telangana, India

⁵Assistant Professor, Department of ECE, CMR Institute of Technology, Hyderabad, Telangana, India

¹srao_allanki@cjits.org, ²madhukumarvanteru@gmail.com, ³azmerachandunaik@cvr.ac.in, ⁴vkvaigandla@gmail.com, ⁵krk.wgl@gmail.com

Abstract— Filter Bank Multicarrier with Offset Quadrature Amplitude Modulation(FBMC/OQAM) system design based on frequency sampling prototype filter takes into account the low frequency utilization of Orthogonal Frequency Division Multiplexing(OFDM) caused by adding Cyclic Prefix(CP). The CP decreases spectral efficiency and increases Peak to Average Power Ratio(PAPR). FBMC is an OFDM enhancement. In this paper to reduce the PAPR, we explained companding methods. We have proposed an FBMC that makes use of prototype pulse shaping filters which can be adjusted to meet system requirements in order to defeat these limitations. Due to its significant effect on the performance of FBMC-OQAM, choosing the right filter is crucial. Different prototype filters are used to investigate the performance of the FBMC-OQAM in this paper. Using the validated system, it was found that frequency utilization is more and good out-band suppression as well as an excellent application value in 5G technology. By using μ -law companding method, FBMC/OQAM provides better performance. It produces low PAPR, low out of band(OoB), high BER performance, less computational complexity and high spectral efficiency as compared to other methods.

Keywords- BER, Companding, CP, FBMC-OQAM, OFDM, PAPR, Pulse Shape, 5G

I. INTRODUCTION

For next generation wireless networks(5G) and standards, FBMC-OQAM is an appropriate multicarrier waveform approach. For different mobile communication services, such as voice communications and data communications, the demand for higher data rates has been increasing day-to-day [1]. Through the development of different generations of mobile technology, from 2G and 3G to 4G and Long-Term Evolution (LTE), mobile technologies have evolved. Future devices will be capable of interacting with machines as well. The development of air interfaces of various technologies has responded to this continuous demand for more data rate [2-3]. In wireless communications, CP-OFDM has proven to be the most reliable type of modulation because of its less complexity. But it has high Out-of-Band(OOB) spectral leakage, spectral efficiency will be decreases and PAPR is increases [4-5]. OFDM does not use pulse shaping, so spectral leakage occurs. The main drawback of OFDM is high PAPR [6]. Because the CP is dropped in the FBMC-OQAM, and because shaping filters reduce OOB emissions significantly, FBMC-OQAM provides good spectral efficiency and spectral shape [7]. FBMC-OQAM divides the QAM symbol into real and imaginary parts and transmits them at twice the QAM rate.

Therefore FBMC is better for 5G communications [6-7]. According to previous works, researchers focused mostly on comparing CP-OFDM with FBMC with specific pulse shaping filters on wireless channels such as [8-10] with the use of PHYDYAS filters. The typical HPA inverse model compensation approach requires numerous simulations to choose optimal compensation thresholds, which is inconvenient for actual applications, and the algorithm does not lower the PAPR of the OFDM/OQAM signal. By clipping at the transmitter, the approach presented in [11] decreases the PAPR of the OFDM/OQAM signal. A study of pulse shaping filters used in FBMC is presented in [12]. Using OFDM and FBMC with an RRC filter, a comparison is provided in [13]. CP-OFDM and FBMC were compared in [14] using half cosine and EGF filters. The performance of shaping under fixed channel conditions is evaluated for frequency and timing offset in [15]. One of the most major problems with the FBMC is the large amount of PAPR due to the high dynamic range of the multicarrier signal. The paper [16] explained a Modified Forest Optimization Algorithm(MFOA) algorithm based on Selected Mapping(SLM), to minimize PAPR and required Bit Error Rate (BER). Studies of the PHYDYAS filter in [17], the Hermite function filter in [18], and the IOTA filter in [19] address the FBMC specific shaping filters.

II. FBMC-OQAM SYSTEM

The FBMC method uses a nonrectangular pulse shaping filter to filter each subcarrier of a multicarrier waveform. As a result, the FBMC symbol overlaps with K (overlapping factor) consecutive FBMC symbols [20], resulting in a prolonged FBMC symbol. The FBMC-OQAM transceiver is shown in Figure 1. A polyphase network (PPN)-FFT implementation and a FS-FBMC implementation are the two types of FBMC implementations. A time-domain subcarrier multiple-tap equalization is used in the PPN-FFT FBMC receiver, causing transmission delays. Each subcarrier is equalized in the frequency domain by the FS-FBMC receiver with no additional delay. FS-FBMC requires larger IFFTs and FFTs of the type KM, M denoting the number of subcarriers. IFFT and FFT of size M are required for the PPN-FFT transceiver, but additional multiplication operations are needed for the KM operation [21].

The FBMC-OQAM system specifically addresses the needs of the sender as described below. After serial high speed data is channel coded and symbol mapped, OQAM is used to modulate the symbols. OQAM preprocessing is designed to maintain subcarrier orthogonality [45]. Subcarriers are formed by dividing the interleaved delay into its real and imaginary components. At sampling time, any subcarriers have an orthogonal distribution, as do adjacent subcarriers. A prototype filter bank with varying offsets is then filtered using the transmission symbols. A fast multi-carrier modulation is then achieved by superimposing the time-domain synthesized signals [22-23]. Pre-processing on the transmitter side converts complex input data $D_{a,b}$ to real symbols. The real and imaginary components of $D_{a,b}$ are then up-sampled by a factor of two [24].

$$D_{a,b}^R = \begin{cases} R\{D_{a,b/2}\}; & \text{b-even} \\ 0; & \text{otherwise} \end{cases} \tag{1}$$

$$D_{a,b}^I = \begin{cases} I\{D_{a,b/2}\}; & \text{b-even} \\ 0; & \text{otherwise} \end{cases} \tag{2}$$

As a result, the $T_{a,b}$ sent symbol will be a mix of real and imaginary parts.

$$T_{a,b} = T_{a,b}^R + T_{a,b}^I \tag{3}$$

In the SFB, the transmitted symbol $T_{a,b}$ is up-sampled by a factor N/2. The filtered signal is then obtained by applying the

procedure of filtration to each subcarrier using a shifted version of the $f_a(k)$.

$$s(k) = \sum_{b=-\infty}^{\infty} \sum_{a=0}^{N-1} T_{a,b} f_a\left(k - \frac{bN}{2}\right) \tag{4}$$

Here, $f_a(k) = e^{\frac{j2\pi ka}{N}} f(k)$ (5)

In the AFB, the demodulated symbol $Y_{a,b}$ may be produced by projecting the received signal $r[k]$ over the receiver filter $\hat{f}_a(k)$.

$$Y_{a,b} = \sum_{k=-\infty}^{\infty} r[k] \hat{f}_a\left(k - \frac{bN}{2}\right) \tag{6}$$

$$\hat{f}_a(k) = f_a^*(k) = e^{-\frac{j2\pi ka}{N}} f(k) \tag{7}$$

The received signal can be expressed as

$$Y_{a,b} = T_{a,b} + j I_{a,b} \tag{8}$$

Here interference is,

$$I_{a,b} = \sum T_{a,b} f_a\left(k - \frac{bN}{2}\right) \hat{f}_a\left(k - \frac{Nb}{2}\right) \tag{10}$$

In [24], the representation matrix of the system model is simplified. The Prototype Filter(PF) may be written as $P \in D^{1*AB}$

$$P = [p_{1,1}, \dots, p_{A,1}, p_{1,2}, \dots, p_{A,B}] \tag{11}$$

The transmitted symbols can be expressed as

$$T = [T_{1,1}, T_{1,2}, \dots, T_{a,1}, T_{1,2}, \dots, T_{a,a}]^T \tag{12}$$

The transmitted signal $s(t)$ may be rewritten as $S = P.T$

The number of received sampled pulses $r_{a,b} \in D^{1*AB}$ which may also be expressed as

$$R = [r_{1,1}, \dots, r_{A,1}, r_{1,2}, \dots, r_{A,B}] \tag{13}$$

Let the fading channel is Additive white Gaussian noise(AWGN) then $R=P$ and the time variant impulse response is $h(a_t, b)$ and delay in channel is a_t .

Finally, the convolution matrix is given by $[H]_{i,j} = h[i - j, i]$ (14)

The symbols on the receiver can be written as:

$$Y = R^H r; Y = R^H H P T + n \tag{15}$$

Here, the received signal $r \in D^{B*1}$, noise from the Gaussian distribution is $n \sim D B(0, g_n R^H R)$ and the power of the time white Gaussian noise is g_n .

Filter banks Multicarrier have the following benefits:

1. No need of the CP.
2. With FBMC, the spectrum is more efficiently used and the system is more selective.
3. Adaptable high determination range used for preparing recipient information flags can be utilized in a similar way.

4. Detection and transmission of exceptional range.
5. Provide strong narrowband jammers.

Filter bank multicarrier has the following disadvantages:

1. Complexity of computation and multifaceted nature.
2. With high data transfer capacity and high element performance, analog radio recurrence execution serves as a key component for usage nonspecific range detection.
3. FBMC can be complicated to implement.
4. Time domain symbol overlapping introduces an overhead.

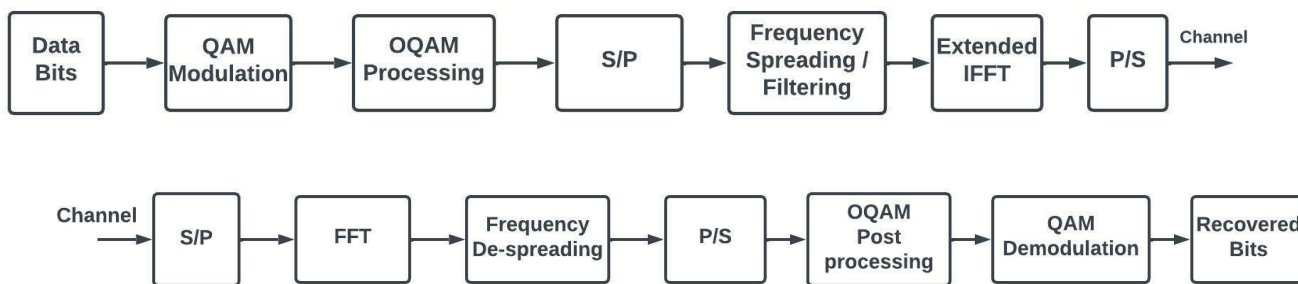


Figure 1. FBMC-OQAM Transceiver

III. PROTOTYPE FILTERS

The filter used in FBMC-OQAM has a higher spectral efficiency and is capable of good OoB suppression. The PPN of FBMC-OQAM systems is generally determined by a prototype filter. This prototype filter gives the attenuation level of each subchannel and overall performance of the system. The frequency sampling method is used to design the prototype filter [25]. Through use of the filter's frequency domain response expression, better sampling points can be designed in the frequency domain, with IFFT providing the time domain value of the filter.

Raised Cosine Filter (RCF): To minimize inter symbol interference (ISI), the RCF is used. According to [26], the impulse response of this filter is

$$f_{RC}(t) = \text{sinc}\left(\frac{t}{T}\right) \left[\frac{\cos(2\Pi at)}{1 - \left(\frac{2at}{T}\right)^2} \right] \tag{16}$$

The roll-off factor a is in this pulse shaping filter. This pulse shaping filter has an asymptotic decay rate of t^3 .

Root Raised Cosine Filter (RRC): As a transmission and receiving filter, RRC is mostly utilized in digital communication. The impulse response of RRC can be found in [27]. For intervals $\pm T$, this filter does not produce a zero response. When $a=0$, this filter gives a zero at $\pm T$.

$$RRC(t) = \frac{\text{Sin}\left(\frac{\Pi t(1-a)}{T}\right) + \left(\frac{4at}{T}\right) \text{Cos}\left(\frac{\Pi t(1+a)}{T}\right)}{\Pi t \left[1 - \left(\frac{4at}{T}\right)^2 \right]} \tag{17}$$

Beter Than Raised Cosine Filter (BTRC): In [28-29], a pulse shaping filter is described along with its impulse response. This filter has a t^2 asymptotic decay rate.

$$BTRC(t) = \text{sinc}\left(\frac{t}{T}\right) \left[\frac{\frac{2t\sigma \sin\left(\frac{\Pi at}{T}\right)}{T} + 2 \cos\left(\frac{\Pi at}{T}\right) - 1}{1 + \left(\frac{\sigma t}{T}\right)^2} \right] \tag{18}$$

Here $\sigma = \frac{\ln(2)}{a B}$; B is bandwidth.

Modified Bartlett Hanning Filter (MBH): This pulse shape's impulse response is described below. According to [30], this pulse shape is given. The window factor σ values varies from 0.5 to 1.88 in this pulse shape.

$$MBH(t) = \text{sinc} \left(\frac{t}{T} \right) \left[\frac{2(1-\sigma) \cos \left(\frac{\Pi at}{T} \right) - 2(1-\sigma) \sin \left(\frac{\Pi at}{T} \right)}{1 - \left(\frac{2at}{T} \right)^2} \right] \quad (19)$$

Improved Sinc Power Shaping Filter (ISP): In [31] this improved pulse is explained. This enhanced pulse's impulse response is given by

$$ISP(t) = e^{-\frac{mt^2}{T^2}} \text{sinc} \left(\frac{t}{T} \right) \quad (20)$$

Here m is the specified parameter and x is the sinc power. The roll-off factor has no effect on the impulse response of this pulse shape [32].

Phase Modified Sinc Pulse (PMSP): In [33] presents this pulse shape, and its time representation is described by,

$$PMSP(t) = e^{-\frac{mt^2}{T^2}} \frac{\sin \left(\frac{(\Pi t - d \sin(p\Pi t))}{T} \right)}{(\Pi t - d \sin(p\Pi t))} \quad (21)$$

where m determines the amplitude, n and p determine the phase, and d gives the degree of the sinc function. The roll-off factor has no effect on the impulse response of this pulse shape.

Parametric Linear Pulses (PLP): The Nyquist ISI-Free Pulses family has a parametric construction [34], and the PLP filter is provided by

$$PLP(t) = \text{sinc} \left(\frac{t\Pi}{T} \right) \text{sinc} \left(\frac{at\Pi}{dT} \right) \quad (22)$$

The PLP has a lower temporal jitter sensitivity than the RC pulse because its asymptotic decay rate is proportional to t^d . The magnitude of the first two sidelobes has the biggest influence on PAPR and mistake probability, according to [35-36]. When striving to decrease transmission mistakes, selecting the suitable filters depending on their rate of decay is a must. The filter that reduces PAPR has relatively few sidelobes in its temporal response, according to the findings of [37]. As a result, by choosing the appropriate decay rate for the filter, we may decrease the PAPR of the system by limiting the energy stored in the tails.

Linear Combination Pulses (LCP): The improved Nyquist pulses may be made by linearly mixing ISI-free pulses with variable decay rates. These pulses have a novel design parameters, the linear combination constant, which provides an extra degree of freedom to decrease inaccuracy in the event of timing faults [32]. The LCP pulses feature more components, such as g or m , which allows for greater flexibility in designing a better performing pulse. Furthermore, the bandwidth (BW) of the pulse generated by linearly mixing two pulses in the spectral domain that totally overlap is the same as the BW of the component pulses. The combined pulse will also meet the Nyquist-I requirement if the combining pulses are ISI-free [37].

The LCP is produced by linearly mixing the RC and PLP pulses, and this pulse's time representation may be defined as

$$LCP(t) = g PLP_{n=1}(t) + (1-g) RC(t)$$

$$LCP(t) = \text{sinc} \left(\frac{\Pi t}{T} \right) \left[g \text{sinc} \left(\frac{\Pi at}{T} \right) + \frac{(1-g) \cos \left(\frac{\Pi at}{T} \right)}{1 - \left(\frac{at}{T} \right)^2} \right] \quad (23)$$

The constant g is selected to lower the corresponding magnitude of the largest side-lobes and diminish OoB emissions [34]. The Nyquist-I condition is met when the LCP preserves the zero ISI situation.

The **Parametric Linear combination pulses (PLCP)** is a linear combination pulse that is created by mixing two PLP pulses with varying degrees of intensity. The combining parameter m , like the LCP, adds an extra degree of freedom that can help decrease errors caused by symbol time problems. The PLCP is also ISI-free, due to two PLP pulses are ISI-free and can be described by

$$PLCP(t) = m PLP_{n=1}(t) + (1-m) PLP_{n=2}(t) \quad (24)$$

$$PLCP(t) = \text{sinc} \left(\frac{\Pi t}{T} \right) \left[\frac{4(1-m) \sin^2 \left(\frac{\Pi at}{2T} \right) + \frac{\Pi amt}{T} \sin \left(\frac{\Pi at}{T} \right)}{\left[\frac{\Pi at}{T} \right]^2} \right] \quad (25)$$

PHYDYAS Filter (PF) : The PF was proposed in [38] and studied in [39]. The PF was then employed in the European PHYDYAS FBMC project [40]. This filter contains filter frequency taps of 2K-1 [41]. The PHYDYAS filter's continuous frequency response is as follows:

$$f(w) = \sum_{a=-k+1}^{k-1} H_a \frac{\sin \left(\Pi mk \left\{ w - \frac{a}{mk} \right\} \right)}{mk \sin \left(\Pi \left\{ w - \frac{a}{mk} \right\} \right)} \quad (26)$$

The continuous frequency domain is denoted by w . H_a coefficients are $f(w)$ values tuned and retrieved at certain frequencies throughout the design process [40]. The equation of the impulse response is

$$P(t) = 1 + 2 \sum_{a=0}^{k-1} H_a \cos\left(\frac{2\Pi at}{kT}\right) \quad (27)$$

Hermite Filter : This is obtained by linearly mixing the Hermite Gaussian function that meets the Nyquist-I condition [42]. As a result, Hermite polynomials in [42] produce the Hermite PF coefficients. The impulse response of the Hermite filter may be characterized as follows:

$$h(t) = \frac{1}{\sqrt{T}} e^{-\frac{2\Pi t^2}{T^2}} \sum_k a_k H_k\left(\frac{2t\sqrt{\Pi}}{T}\right) \quad (28)$$

IV. PAPR MINIMIZATION METHODS

A linear amplifier with a large input imposes nonlinear distortion on its output because of its saturation characteristics caused by a large input. P_o^{\max} limits the maximum possible output of the amplifier due to the saturation characteristics.

$$\text{Input Back-Off (IBO)} = 10 \log_{10} \left(\frac{P_i^{\max}}{p_i} \right) \quad (29)$$

$$\text{Output Back-Off (OBO)} = 10 \log_{10} \left(\frac{P_o^{\max}}{p_o} \right) \quad (30)$$

When a high input is used to stimulate the nonlinear feature of an HPA (High Power Amplifier), it creates out-of-band radiation that impacts transmissions in neighboring bands, as well as in-band distortions that induce rotation, attenuation, and offset on the received signal [43].

PAPR is the ratio of the signal's maximum and average power.

$$PAPR = \frac{\text{Max.Power}}{\text{Avg.Power}} \quad (31)$$

$$x(t)_{PAPR} = \frac{\text{Max}|x(t)|^2}{E[|x(t)|^2]} \quad (32)$$

Power amplifiers must operate at a lower power efficiency due to the high PAPR FBMC signal. Consequently, mobile devices' battery life decreases [44]. For the FBMC signal the PAPR can be represented as

$$[x(n)_{PAPR}]_{db} = 10 \log_{10} \left(\frac{\text{Max}|x(n)|^2}{E[|x(n)|^2]} \right) \quad (33)$$

μ -law companding : The FBMC signal with μ -law companded may be written as

$$H(x_n) = \text{sgn}(x_n) \frac{\log(1 + \mu|x_n|)}{\log(1 + \mu)} \quad (34)$$

The signal representation of inverse μ -law companded is

$$H^{-1}(r_n) = \left[(1 + \mu)^{|r_n|} - 1 \right] \frac{\text{sgn}(r_n)}{\mu} \quad (35)$$

The companding parameter is μ , the received companded FBMC signal is r_n and the signum function is sgn .

A-law Companding : The FBMC signal with A-law companded is given by

$$H(x_n) = \frac{A|x_n|\text{sgn}(x_n)}{1 + \log A}; |x_n| < \frac{1}{A} \quad (36)$$

$$H(x_n) = \frac{[1 + \log(A|x_n|)]\text{sgn}(x_n)}{1 + \log A}; \frac{1}{A} \leq |x_n| < 1 \quad (37)$$

The signal representation of inverse A-law companded is

$$H^{-1}(r_n) = \frac{(1 + \log A)|r_n|\text{sgn}(r_n)}{A}; |r_n| < \frac{1}{1 + \log A} \quad (38)$$

$$H^{-1}(r_n) = \frac{e^{[(1 + \log A)|r_n| - 1]}}{A}; \frac{1}{1 + \log A} \leq |r_n| < 1 \quad (39)$$

Here companding parameter is A.

Rooting Companding : The FBMC signal with rooting companded is described as

$$H(x_n) = \text{sgn}(x_n)|x_n|^R \quad (40)$$

The signal representation of inverse rooting companded is

$$H^{-1}(r_n) = \text{sgn}(r_n)|r_n|^{\frac{1}{R}} \quad (41)$$

Here companding parameter is R and varies from 0.1 to 0.9.

Tangent Rooting Companding : FBMC signal with tangent rooting companding is given by

$$H(x_n) = \text{sgn}(x_n) \text{Tanh} \left[\left(|x_n| T \right)^R \right] \quad (42)$$

The inverse companded signal with tangent rooting is

$$H^{-1}(r_n) = \text{sgn}(r_n) \left| \text{Tanh} \left[\frac{|r_n|}{T} \right]^{\frac{1}{R}} \right| \tag{43}$$

The companding parameters are T and R. T varies from 5 to 25 and R varies from 0.1 to 1.

Logarithmic Rooting Companding : FBMC signal with logarithmic rooting companded can be given as

$$H(x_n) = \text{sgn}(x_n) \log_e \left[(|x_n L|)^R \right] \tag{44}$$

The inverse companded signal with logarithmic rooting companded is

$$H^{-1}(r_n) = \text{sgn}(r_n) \left[e^{\frac{|r_n|}{L}} \right]^{\frac{1}{R}} \tag{45}$$

The companding parameters are L and R.

Error Function Companding : FBMC signal with error function companded is

$$H(x_n) = e_1 \text{erf}(e_2 P_k) \tag{46}$$

The inverse companding is calculated as follows:

$$H^{-1}(r_n) = \frac{2e_1 e_2}{\sqrt{\pi}} e^{\left[-(e_2 r_n)^2 \right]} \tag{47}$$

Here $e^{\left[-(e_2 r_n)^2 \right]} \leq 1$; and $H^{-1}(r_n) < Z$ where $Z > \frac{2e_1 e_2}{\sqrt{\pi}}$

where P_k is output of poly phase network and these companding parameters e_1, e_2 control how much companding level will be applied, and they must be positive.

V. SIMULATION RESULTS

The effectiveness of the suggested prototype pulse shaping filters in FBMC/OQAM systems is investigated in this section. Simulations were performed using MATLAB and simulation values are represented in table 1. We examined the effectiveness of the FBMC/OQAM system using various companding methods. We analyze the pulse shaping filters in terms of impulse response and frequency response. The results may be utilized to identify a well-localized pulse in both the time and frequency domains. FBMC/OQAM is a waveform well suited to the next generation of wireless communication systems, since it provides high spectral efficiency as well as low OoB emissions.

Table1 . Simulation parameters

Parameters	Value
Simulation tool	MATLAB
subcarriers M	2048
Overlapping factor K	2, 3, 4
Filter length	1024
Modulation	QAM
Channel	AWGN
Subcarrier bandwidth	15 KHz
Roll-off factor	0.5
filter	PHYDYAS

The PSD of FBMC as shown in figure 2 and the magnitude response is illustrated in figure 3. The OoB leakage of the FBMC-OQAM is extremely low. As the filter coefficients are increased in the FBMC, the side band is further suppressed. As these coefficients increase, both transmitters and receivers become more complex. The FBMC is more efficient, but it has complexity. The impulse response and frequency response of the most widely used pulse shapes is illustrated in figure 4 and figure 5, respectively.

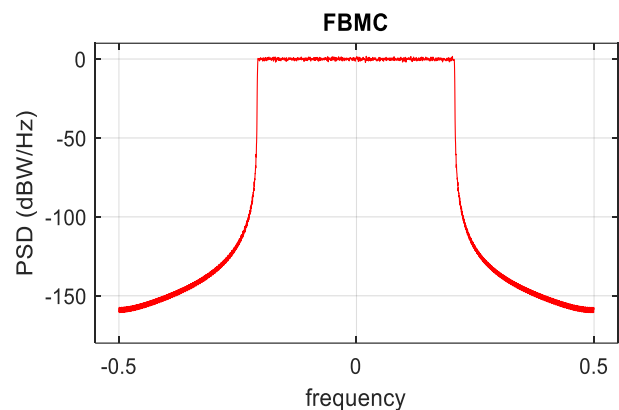


Figure 2. FBMC : PSD

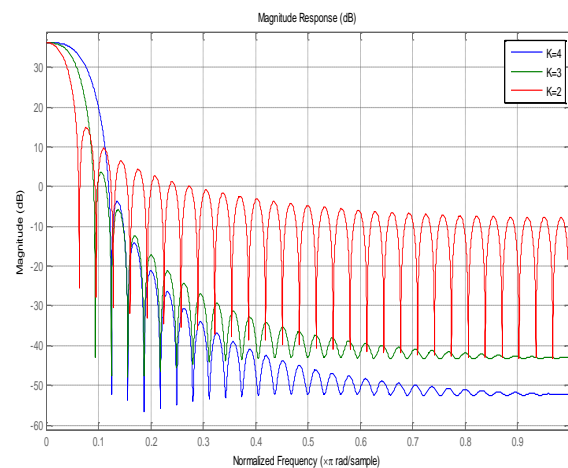


Figure 3. Magnitude response

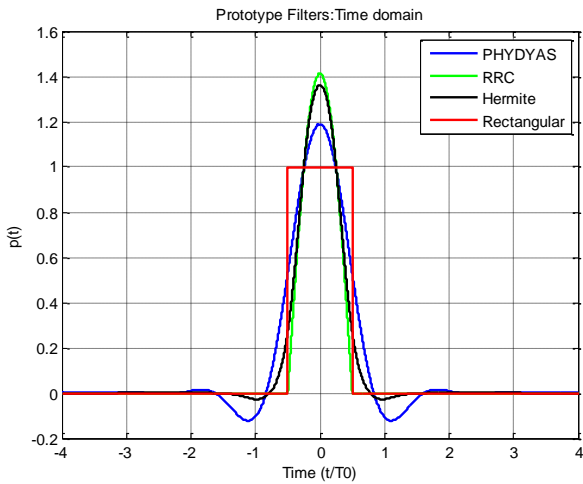


Figure 4. Time Response

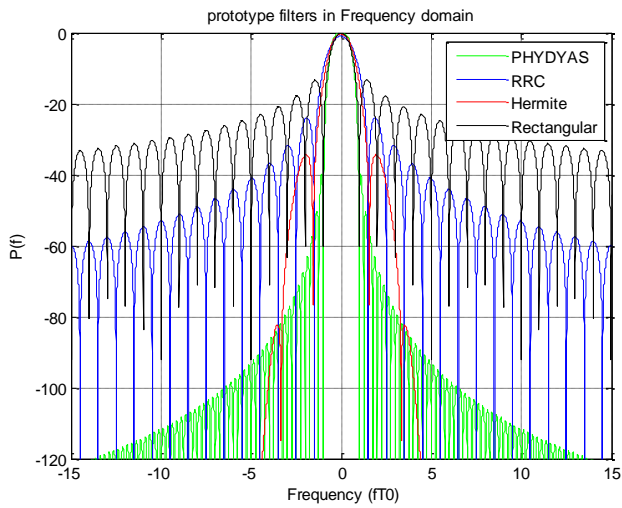


Figure 5. Frequency Response

The figure 6 illustrates the PAPR of the FBMC-OQAM for various subcarrier. This indicates that the PAPR of the system increases with the amount of subcarriers increases. When the subcarriers are 128 the PAPR is 6.6dB and for the subcarriers 512, 1024 and 2048 the PAPR values are 10.2dB, 11.1dB and 12dB, respectively. The results shows that PAPR is less as the subcarriers are less.

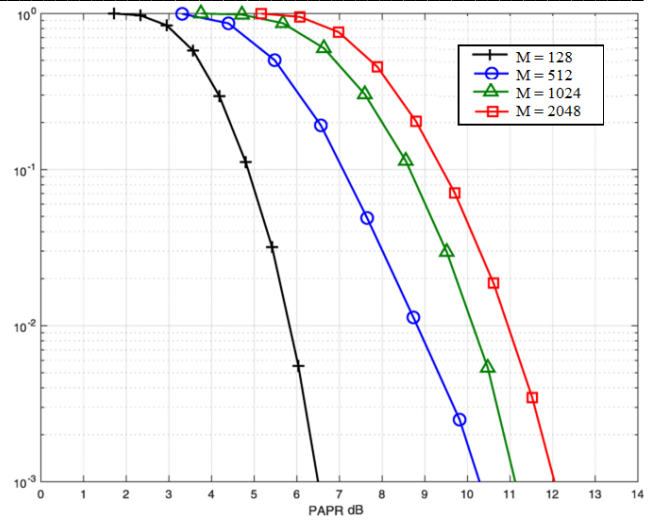


Figure 6. PAPR for various subcarriers

For different values of the overlapping factors(K), the PAPR of the FBMC-OQAM can be observed in figure 7. With increasing values of the overlapping factor, the PAPR also increases. Because, increasing K results in a larger extended IFFT and more symbols overlapping simultaneously. For the original signal the PAPR is 10.9 dB. At a CCDF of 10^{-3} the overlapping factors are 4, 3 and 2, then the PAPR values are 9.4dB, 9dB and 6.4dB, respectively. For the lower overlapping factor value, the system gives lower PAPR and provides better performance.

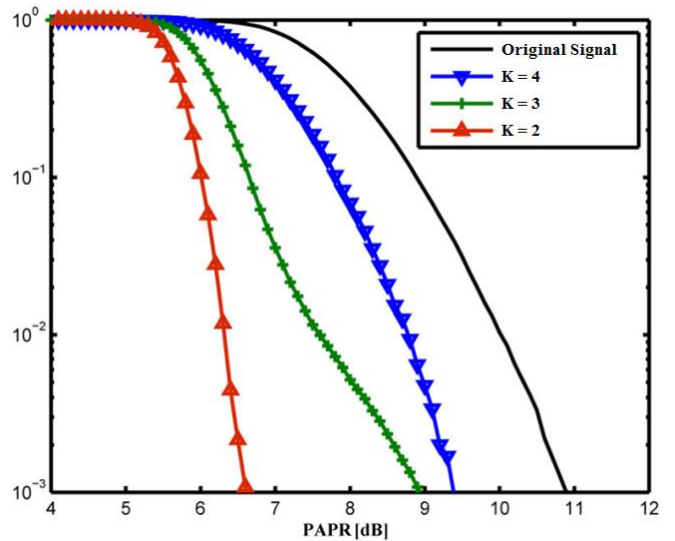


Figure 7. PAPR for various overlapping factor

Figure 8 shows the simulated CCDF at the different companding techniques as a function of the PAPR. . For the original signal the PAPR is 10.9 dB. At a CCDF of 10^{-3} the PAPR values are 6.1dB, 7.1 dB, 7.2dB, 7.9dB, 8.8dB for μ -law companding, A-law companding, error function companding, logarithmic rooting companding and tangent rooting companding, respectively. The PAPR of μ -law companding, A-law companding, error function companding,

logarithmic rooting companding and tangent rooting companding are reduced with 4.8dB, 3.8dB, 3.7dB, 3dB and 2.1dB as compared with original signal. The μ -law companding method provides lower PAPR and better performance.

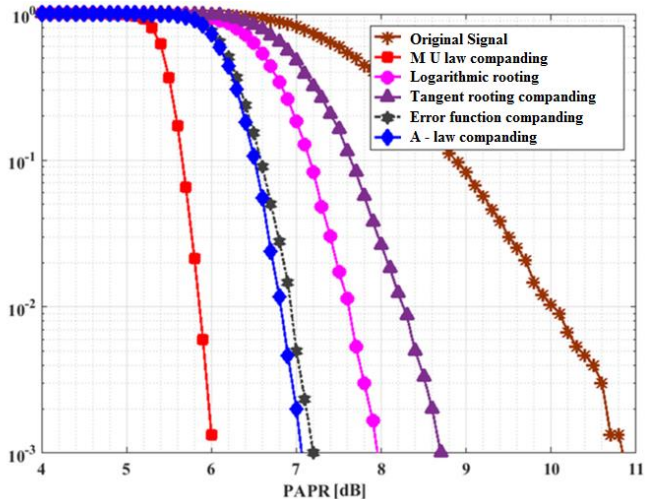


Figure 8. PAPR with various companding methods

Figure 9 displays the BER in relation to SNR for different companding approaches. At a BER of 10^{-7} , the SNR values are 5.2dB, 6.3dB, 7.4dB, 8.1dB and 10.2dB for μ -law companding, A-law companding, error function companding, logarithmic rooting companding and tangent rooting companding, respectively. The μ -law companding method provides better BER performance.

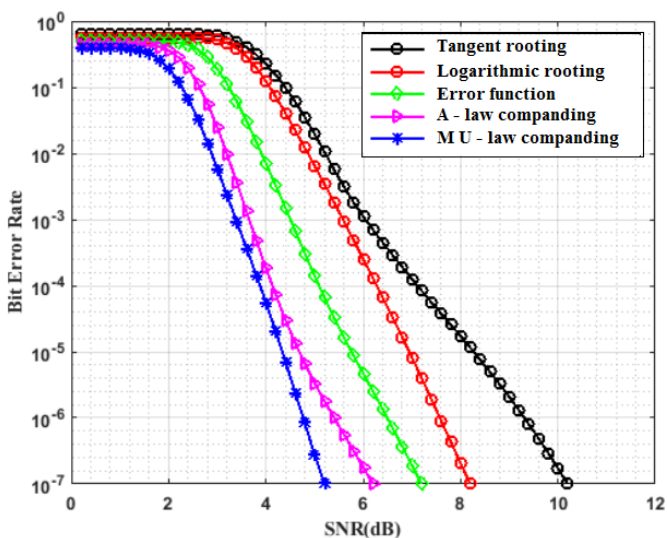


Figure 9. BER performance of various companding methods

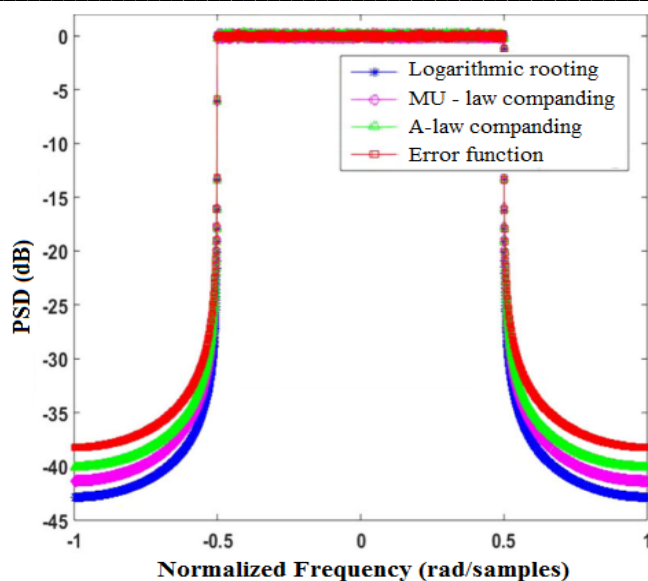


Figure 10. PSD

Figure 10 represents the PSD performance of PAPR minimization techniques in order to analyze out of band interference (OBI). Normally PSDs are calculated using a periodogram. As the distortion increases, the power OoB emission also increases. According to Figure 10, μ -law companding delivers 1.24dB and 3.21dB lower OBI than A-law and error function companding and 1.4dB more OBI than logarithmic rooting.

VI. CONCLUSION

A benefit of FBMC systems to CP-OFDM is that they are more spectrally efficient, allow for dynamic spectrum allocation, and are less susceptible to carrier frequency offset (CFO). By studying transmultiplexers mathematically, polyphase filter banks are developed that are computationally more efficient than lattice structures, significantly improving spectral efficiency when combined with OQAM. The benefits of the FBMC-OQAM system include strong spectrum OoB suppression, low CP requirements, great spectrum efficiency, no need for carrier synchronization, and suitability for fragmented spectrum usage. The prototype filter developed in this study has a high practicability and may be employed in a 5G MC transmission FBMC/OQAM system. Different Prototype pulse shape filters are described in this study to enhance performance of FBMC/OQAM systems. In this paper we analyzed the PAPR change caused by the no. of subcarriers. Various methods of reducing PAPR have been studied. Companding techniques effectively decreases the PAPR, however the subcarrier selection is also a significant factor in decreasing PAPR.

DECLARATION OF COMPETING INTEREST

The authors declare that there is no conflict of interest regarding the publication of this paper.

FUNDING DECLARATION

No funding.

REFERENCES

[1] Karthik Kumar Vaigandla, "Communication Technologies and Challenges on 6G Networks for the Internet: Internet of Things (IoT) Based Analysis," *2022 2nd International Conference on Innovative Practices in Technology and Management (ICIPTM)*, 2022, pp. 27-31, doi: 10.1109/ICIPTM54933.2022.9753990.

[2] Kommabatla Mahender, Tipparti Anil Kumar, K. S. Ramesh, "Analysis of multipath channel fading techniques in wireless communication systems," *AIP Conference Proceedings* 1952, 020050 (2018); <https://doi.org/10.1063/1.5032012>

[3] Karthik Kumar Vaigandla, J.Benita, "PRNGN - PAPR Reduction using Noise Validation and Genetic System on 5G Wireless Network," *International Journal of Engineering Trends and Technology*, vol. 70, no. 8, pp. 224-232, 2022. Crossref, <https://doi.org/10.14445/22315381/IJETT-V70I8P223>

[4] Mohammed Kasim Al-Haddad, Hadi T. Ziboon, "Comparative Study of Pulse Shaping Filters in FBMC," *Iraqi Journal of Computers, Communications, Control, and Systems Engineering*, 2019, Volume 19, Issue 2, Pages 30-40

[5] Karthik Kumar Vaigandla, Dr.J.Benita, "Study and Analysis of Various PAPR Minimization Methods," *International Journal of Early Childhood Special Education (INT-JECS)*, Vol 14, Issue 03 2022, pp.1731-1740.

[6] Karthik Kumar Vaigandla and B. J, Study and analysis of multi carrier modulation techniques – FBMC and OFDM, Materials Today: Proceedings, <https://doi.org/10.1016/j.matpr.2021.12.584>

[7] Vaigandla, K. K. ., & Benita, J. (2023). A Novel PAPR Reduction in Filter Bank Multi-Carrier (FBMC) with Offset Quadrature Amplitude Modulation (OQAM) Based VLC Systems. *International Journal on Recent and Innovation Trends in Computing and Communication*, 11(5), 288–299. <https://doi.org/10.17762/ijritcc.v11i5.6616>

[8] R. Nissel and M. Rupp "OFDM and FBMC-OQAM in doubly-selective channels: calculating the bit error probability," *IEEE Communications Letters*, Volume. 21, Issue 6, June 2017.

[9] D. Gregoratti and X. Mestre, "Distortion analysis in OQAM/FBMC-based OFDMA" *IEEE 16th International Workshop on Signal Processing Advances in Wireless Communications (SPAWC)*, Stockholm, 2015.

[10] J. Bazzi, P. Weitkemper, K. Kusume, A. Benjebbour, Y. Kishiyama "Design and Performance Tradeoffs of Alternative Multi-Carrier Waveforms for 5G," in *Proc. IEEE Globecom Workshops*, San Diego, Dec. 2015, pp. 1–6.

[11] Karthik Kumar Vaigandla and J.Benita (2022), Novel Algorithm for Nonlinear Distortion Reduction Based on Clipping and Compressive Sensing in OFDM/OQAM System. *IJEER* 10(3), 620-626. <https://doi.org/10.37391/IJEER.100334>.

[12] Z. Zhao, M. Schellmann, X. Gong, Q. Wang, R. Böhnke and Y. Guo "Pulse shaping design for OFDM systems,"

EURASIP Journal on Wireless Communications and Networking, (2017) 2017:74

[13] M. Xu, J. Zhang, F. Lu, Y. Wang, D. Guidotti, and G. K. Chang, "Investigation of FBMC in mobile fronthaul networks for 5g wireless with time-frequency modulation adaptation," *Optical Fiber Communications Conference and Exhibition (OFC)*, California,

[14] J. Du, and S. Signell "Pulse Shape Adaptivity in OFDM/OQAM Systems," *International Conference of Advanced Infocomm Technology (ICAIT)*, Shen Zhen, China, July 2008.

[15] A. Şahin, İ. Güvenç, and H. Arslan, "A Survey on Prototype Filter Design for Filter Bank Based Multicarrier Communications," *IEEE Communications Surveys & Tutorials*, Dec. 2013.

[16] Vaigandla, Karthik Kumar and Benita, J. 'Selective Mapping Scheme Based on Modified Forest Optimization Algorithm for PAPR Reduction in FBMC System'. *Journal of Intelligent & Fuzzy Systems*, pp. 1-15, 2023, DOI: 10.3233/JIFS-222090.

[17] M. Bellanger, "FBMC physical layer: a primer," *Tech. Rep.* 06/2010, 2010.

[18] R. Haas and J.-C. Belfiore, "A time-frequency well-localized pulse for multiple carrier transmission," *Wireless Pers. Commun.*, vol. 5, pp. 1–18, 1997.

[19] M. Alard. "Construction of a multicarrier signal," *Patent WO* 96/35278, 1996.

[20] Anam Mobin and Anwar Ahmad, " PAPR and BER analysis of coded FBMC-OQAM system with non-linear companding techniques," *Engineering Research Express* 4 (2022) 025026, <https://doi.org/10.1088/2631-8695/ac6fb4>

[21] BellangerM2012 FS-FBMC: a flexible robust scheme for efficient multicarrier broadband wireless access 2012 *IEEE Globecom Workshops* pp 192–6(Piscataway, NJ) (IEEE)

[22] Ling Yao *et al* 2019 *J. Phys.: Conf. Ser.* 1213 052068, doi:10.1088/1742-6596/1213/5/052068

[23] Kommabatla Mahender, Tipparti Anil Kumar and K S Ramesh, "An Efficient FBMC Based Modulation For Future Wireless Communications," *ARPN Journal of Engineering and Applied Sciences*, VOL. 13, NO. 24, December 2018, pp. 9526-9531

[24] J. M. Choi, Y. Oh, H. Lee, and J. S. Seo, "Pilot-Aided Channel Estimation Utilizing Intrinsic Interference for FBMC/OQAM Systems," *IEEE Trans. Broadcast.*, vol. 63, no. 4, pp. 644–655, 2017.

[25] Umamaheshwar Soma and Kommabatla Mahender, " PAPR reduction based on subcarriers in FBMC based system," *AIP Conference Proceedings* 2418, 030069 (2022); <https://doi.org/10.1063/5.0081692>

[26] K. Gentile, "The care and feeding of digital pulse-shaping filters," *RF Des.*, vol. 25, no. 4, pp. 50_58, 2002.

[27] N. S. Alagha and P. Kabal, "Generalized raised-cosine filters," *IEEE Trans. Commun.*, vol. 47, no. 7, pp. 989_997, Jul. 1999.

[28] S. D. Assimonis, M. Matthaiou, G. K. Karagiannidis, and J. A. Nossek, "Optimized 'better than' raised-cosine pulse for reduced ICI in OFDM systems," in *Proc. 17th Int. Conf. Telecommun.*, Doha, Qatar, Apr. 2010, pp. 249_252.

- [29] N. C. Beaulieu, C. C. Tan, and M. O. Damen, "A better than Nyquist pulse," *IEEE Commun. Lett.*, vol. 5, no. 9, pp. 367-368, Sep. 2001.
- [30] J. K. Gautam, A. Kumar, and R. Saxena, "On the modified bartlettthanning window (family)," *IEEE Trans. Signal Process.*, vol. 44, no. 8, pp. 2098-2102, Aug. 1996.
- [31] V. Kumbasar and O. Kucur, "ICI reduction in OFDM systems by using improved sinc power pulse," *Digit. Signal Process.*, vol. 17, no. 6, pp. 997-1006, Nov. 2007
- [32] HEBA M. ABDEL-ATTY, WALID A. RASLAN, AND ABEER T. KHALIL, " Evaluation and Analysis of FBMC/OQAM Systems Based on Pulse Shaping Filters," *IEEE Access*, VOLUME 8, 2020, DOI: 10.1109/ACCESS.2020.2981744
- [33] A. L. Onofrei and N. D. Alexandru, "The effect of ICI in OFDM systems using improved phase modified sinc pulse," in *Proc. Int. Symp. Signals, Circuits Syst.*, Iasi, Romania, Jul. 2009, pp. 1-4.
- [34] N. C. Beaulieu and M. O. Damen, "Parametric construction of Nyquist- I pulses," *IEEE Trans. Commun.*, vol. 52, no. 12, pp. 2134-2142, Dec. 2004.
- [35] J. O. Scanlan, "Pulses satisfying the Nyquist criterion," *Electron. Lett.*, vol. 28, no. 1, pp. 50-52, Jan. 1992.
- [36] B. Farhang-Boroujeny, "A square-root Nyquist (M) filter design for digital communication systems," *IEEE Trans. Signal Process.*, vol. 56, no. 5, pp. 2127-2132, May 2008.
- [37] P. Sandeep, S. Chandan, and A. K. Chaturvedi, "ISI-free pulses with reduced sensitivity to timing errors," *IEEE Commun. Lett.*, vol. 9, no. 4, pp. 292-294, Apr. 2005.
- [38] S. Mirabbasi and K. Martin, "Design of prototype filter for near-perfect-reconstruction overlapped complex-modulated transmultiplexers," *2002 IEEE International Symposium on Circuits and Systems. Proceedings (Cat. No.02CH37353)*, 2002, pp. I-I, doi: 10.1109/ISCAS.2002.1009967.
- [39] S. Mirabbasi and K. Martin, "Overlapped complex-modulated transmultiplexer filters with simplified design and superior stopbands," *IEEE Trans. Circuits Syst. II. Analog Digit. Signal Process.*, vol. 50, no. 8, pp. 456-469, Aug. 2003
- [40] M. Bellanger, D. Le Ruyet, D. Roviras, M. Terré, J. Nossek, L. Baltar, Q. Bai, D. Waldhauser, M. Renfors, and T. Ihalainen, "FBMC physical layer: A primer," *Phydyas*, vol. 25, no. 4, pp. 7-10, 2010.
- [41] M. G. Bellanger, "Specification and design of a prototype filter for filter bank based multicarrier transmission," in *Proc. IEEE Int. Conf. Acoust., Speech, Signal Process.*, Salt Lake City, UT, USA, May 2001, pp. 2417-2420.
- [42] R. Haas and J.-C. Belfiore, "A time-frequency well-localized pulse for multiple carrier transmission," *Wireless Pers. Commun.*, vol. 5, no. 1, pp. 1-18, Jan. 1997.
- [42] Mahmood Jasim Mohammed and Abd Al Kareem Ali Mohammed 2021 *J. Phys.:Conf. Ser.* 1973 012098, doi:10.1088/1742-6596/1973/1/012098
- [43] Kommabatla Mahender , Tipparti Anil Kumar , K.S Ramesh, "PAPR Analysis of Fifth Generation Multiple Access Waveforms for Advanced Wireless Communication," *International Journal of Engineering & Technology*, 7 (3.34) (2018) 487-490.
- [44] Karne, R. K. ., & Sreeja, T. K. . (2023). PMLC- Predictions of Mobility and Transmission in a Lane-Based Cluster VANET Validated on Machine Learning. *International Journal on Recent and Innovation Trends in Computing and Communication*, 11(5s), 477-483. <https://doi.org/10.17762/ijritcc.v11i5s.7109>
- [45] Radha Krishna Karne and Dr. T. K. Sreeja (2022), A Novel Approach for Dynamic Stable Clustering in VANET Using Deep Learning (LSTM) Model. *IJEER* 10(4), 1092-1098. DOI: 10.37391/IJEER.100454.